Tissue and Cell 88 (2024) 102417

Contents lists available at ScienceDirect

Tissue and Cell

journal homepage: www.elsevier.com/locate/tice

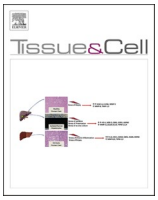

Histological and scanning electron microscope observations on the developing retina of the cuttlefish (*Sepia officinalis* Linnaeus, 1758)

Alejandro Arias-Montecino [a], Antonio Sykes [b], Guadalupe Álvarez-Hernán [c,*], José Antonio de Mera-Rodríguez [a], Violeta Calle-Guisado [c], Gervasio Martín-Partido [a], Joaquín Rodríguez-León [c], Javier Francisco-Morcillo [a]

[a] *Área de Biología Celular, Departamento de Anatomía, Biología Celular y Zoología, Facultad de Ciencias, Universidad de Extremadura, Badajoz 06006, Spain*
[b] *Center of Marine Sciences, Universidade do Algarve Campus de Gambelas, Faro 8005-139, Portugal*
[c] *Área de Anatomía y Embriología Humana, Departamento de Anatomía, Biología Celular y Zoología, Facultad de Medicina, Universidad de Extremadura, Badajoz 06006, Spain*

ARTICLE INFO

Keywords:
Cephalopod
Development
Histogenesis
Retina
Sepia officinalis

ABSTRACT

In this work we present a detailed study of the major events during retinal histogenesis of the cuttlefish *Sepia officinalis* from early embryos to newly hatched animals and juveniles. For this purpose, we carried out morphometric and histological analyses using light and scanning electron microscopy. From St19, the first embryonic stage analysed, to St23/24 the embryonic retina is composed of a pseudostratified epithelium showing abundant mitotic figures in the more internal surface. At St24 the first photoreceptor nuclei appear in the presumptive inner segment layer, while an incipient layer of apical processes of the future rhabdomeric layer become visible at St25. From this stage onwards, both the rhabdomeric layer and the inner segment layer increase in size until postnatal ages. In contrast, the width of the supporting cell layer progressively decreases from St25/26 until postnatal ages. *S. officinalis* embryos hatched in a morphologically advanced state, showing a differentiated retina even in the last stages of the embryonic period. However, features of immaturity are still observable in the retinal tissue during the first postnatal weeks of life, such as the existence of mitotic figures in the apical region of the supporting cell layer and migrating nuclei of differentiating photoreceptors crossing the basal membrane to reach their final location in the inner segment layer. Therefore, postnatal retinal neurogenesis is present in juvenile specimens of *S. officinalis*.

1. Introduction

The eye of cephalopods is a classic example of convergent evolution between an invertebrate and a vertebrate sensory system (Koenig and Gross, 2020). However, comparative studies have shown important anatomical and histological differences (Hanke and Kelber, 2020; Koenig and Gross, 2020; Nilsson et al., 2023). In this sense, the cephalopod retina is everted instead of inverted. Furthermore, while the vertebrate retina has a multilayered structure containing several types of photoreceptors, neurons, and glial cells (Bejarano-Escobar et al., 2014; Kolb et al., 2001) the cephalopod retina is composed of two nuclear layers separated by a basal membrane containing photoreceptors and support cells (Imarazene et al., 2017). More striking differences are found in the comparison of the retinal development between cephalopods and vertebrates. The vertebrate retina originates from bilateral evaginations of the neural tube (Francisco-Morcillo et al., 2014; Moreno-Marmol et al., 2018), but the cephalopod eye develops from bilateral invaginations of the cephalic ectoderm (Harris, 1997; Koenig et al., 2016; Napoli et al., 2022; Tomarev et al., 1997). In the case of cell differentiation in the retinal rudiment, retinal progenitors undergo interkinetic nuclear migration in a pseudostratified epithelium both in cephalopods (Koenig and Gross, 2020; Napoli et al., 2022) and vertebrates (Agathocleous and Harris, 2009; Álvarez-Hernán et al., 2022a; Baye and Link, 2007; Norden, 2017), but during nuclear migration, mitosis takes place in the innermost region of the undifferentiated retina in cephalopods, inverted to that of vertebrates. As development proceeds, asymmetrical divisions produce migratory retinal progenitors that lose contact with the apical surface and migrate radially into the vertebrate

* Correspondence to: Área de Anatomía y Embriología Humana Departamento de Anatomía, Biología Celular y Zoología, Facultad de Ciencias, Universidad de Extremadura, Badajoz 06006, Spain.
E-mail address: galvarezt@unex.es (G. Álvarez-Hernán).

https://doi.org/10.1016/j.tice.2024.102417
Received 29 January 2024; Received in revised form 3 May 2024; Accepted 20 May 2024
Available online 27 May 2024

Table 1
S. officinalis embryos and hatchlings used in the present study. The embryos are given to the developmental stage (St) of Boletzky et al. (2016) and their age (from embryonic day, E10, St19) to the hatching day (E30, St30, postnatal day, P0). Hatchlings at different ages were also included (P7, P14, P21).

Embryonic day (E)	Stage of development (St)	n	Embryonic(E) or posthatch (P) day	Stage of development (St)	n
E10	St19	3	E22	St27	4
E11	St20	3	E23	St28	4
E12	St21	3	E24	St28/29	4
E13	St21/22	3	E25	St29	4
E14	St22	3	E26	St29	4
E15	St22/23	3	E27	St29	4
E16	St23	3	E28	St29/30	4
E17	St23/24	4	E29	St30	4
E18	St24	4	E30-P0	St30	4
E19	St25	4	P7		3
E20	St25/26	4	P14		3
E21	St26	4	P21		3
TOTAL SPECIMENS (n): 86					

neuroepithelium to their final location, where they differentiate in different subtypes of neurons (Petridou and Godinho, 2022). As cell differentiation occurs, the emergence of the retinal layers in the vertebrate retina can also be observed, increasing in thickness with the progression of tissue differentiation (Álvarez-Hernán et al., 2021c). Migrating progenitors in the developing cephalopod retina can only give rise to photoreceptors and they migrate towards the base of the pseudostratified epithelium and move further basally through the basal membrane (Bozzano et al., 2009; Koenig et al., 2016; Yamamoto, 1985a).

Other aspects of visual system development have been described in cephalopods, such as maturation of eye tissues in cuttlefish *Sepiella japonica* (Yamamoto, 1985a), *Octopus australis* (Wentworth and Muntz, 1992), southern calamari *Sepiotheutis australis* (Bozzano et al., 2009), squid *Doryteuthis pealeii* (Koenig et al., 2016), or retinal development in the cuttlefish *Sepia esculenta* (Hao et al., 2010), Cranchiid squid *Teuthowenia pellucida* (Evans et al., 2015), squid *Doryteuthis pealeii* (Napoli et al., 2022) and long arm octopus *Octopus minor* (Ryu et al., 2023).

The European cuttlefish (*Sepia officinalis* Linnaeus 1758) has been identified as a cephalopod species potentially suitable for industrial aquaculture (Sykes et al., 2012, 2006). The development of the *S. officinalis* eye has been investigated in some genomic studies (Buresi et al., 2012, 2013; Imarazene et al., 2017), but the timing of the histogenesis of the retina in this cephalopod species has not been reported in detail. The purpose of the present paper is to provide a qualitative and quantitative detailed description of *S. officinalis* retinal development

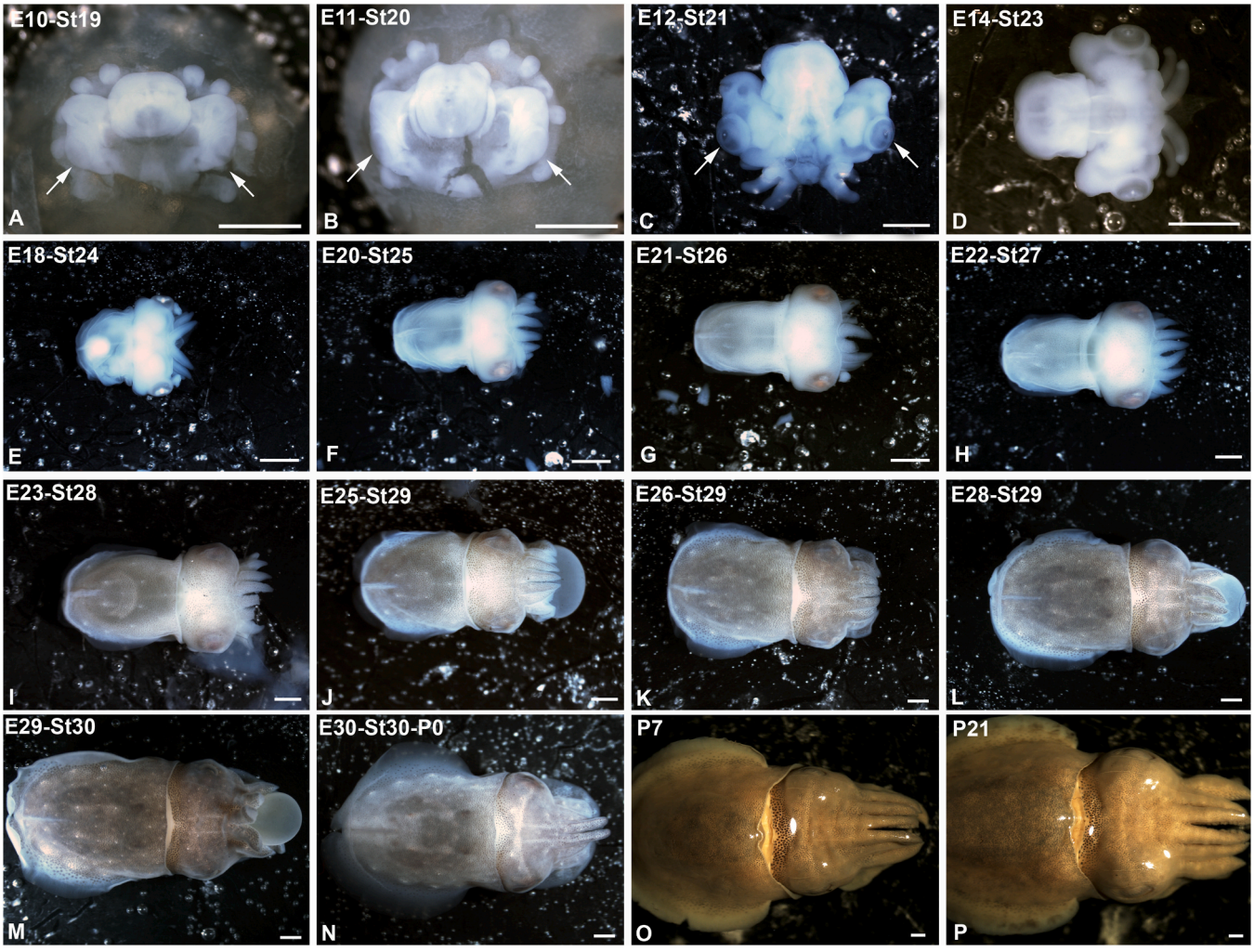

Fig. 1. Stereomicroscope images of some of the *S. officinalis* embryos and post-hatched specimens included in the present study showing the external gross anatomical changes of the eye. The embryos are classified according to the developmental stage (St) of Boletzky et al. (2016), and their age (from embryonic day, E10, St19) to the hatching day (E30, St30, postnatal day, P0). Hatchlings at different ages were also included (P7, P14, P21). Arrows point to the eye in the first developmental stages. *Scale bars: 1 mm.*

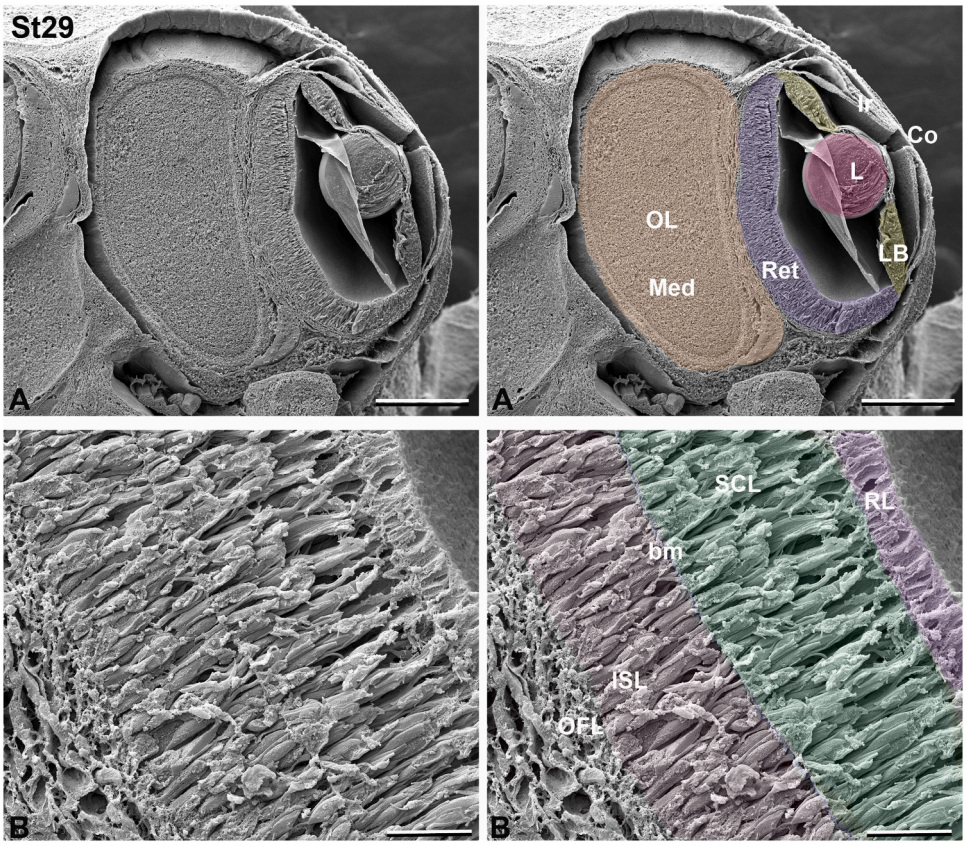

Fig. 2. Scanning electron micrographs of eye balls in a St29 embryo of *S. officinalis*, showing the anatomy of the visual system (A,A) and the histology of the retina (B, B). SEM images (A,B) are digitally coloured (A,B) to clearly distinguish the different regions of the visual system. (A,A) The OpL is located beneath the eye, and the Co, Ir, L, LB and the Ret are clearly visible in the developing eye. (B,B) The laminar structure of the retina is clearly established and the RL, the SCL, the bm, the ISL, and the OFL are clearly visible. *Abbreviations: bm, basal membrane; Co, cornea; Ir, iris; ISL, Inner segmental layer; L, lens; LB; lentigenic body; Med; central medulla; OFL, optic fibre layer; OpL, optic lobe; Ret, retina; RL, rhabdomeric layer; SCL, supporting cell layer. Scale bars: 250 μm in A,A; 25 μm in B,B.*

from early stages of development to early postnatal life, via light and scanning electron microscopic observations.

2. Material and methods

2.1. Experimental animals

All specimens of *S. officinalis* used in the present study originate from a single brood obtained from *F4* cultured females at the *Ramalhete Aquaculture Station* (Ria Formosa, South Portugal - 37°00′22.39″N; 7°58′02.69″W). Eggs were kept in artificial sea water with aeration at controlled temperature (17–19 °C). The length of the embryonic period in cephalopods particularly depends on temperature (Lemaire, 1970; Mangold-Wirz, 1963). In these conditions, the duration of development in *S. officinalis* embryos was 30 days (Buresi et al., 2012). Each day, individual eggs were taken from the aquarium and embryos were extracted using thin clips in filtered sea water. All specimens were anaesthetized in a cold chamber (4 °C) or in ice, observed under a Stereoscopic Microscope SMZ-1000 (Nikon) and photographed using a Digital Camera DS-5Mc (Nikon). Subsequently, the developmental stage of the embryos was ascertained following the criteria outlined by Boletzky et al. (2016). This classification is established using morphological attributes including eye colour and position, arm structure, and the distribution of chromatophores. These stages are based on external anatomical features and numbered from stage 1 (St1) to St30. St30 represents the newly hatched cuttlefish (posthatch day 0, P0) with a completely reduced yolk sac. A total of 73 *S. officinalis* embryos and 13 hatchlings (Table 1) were included in the present study, ranging from St19 to St22, the period of organogenesis (extension phase), and from St23 to St30, the period of organogenesis (growth phase) (Boletzky et al., 2016). Fig. 1 shows embryos representing various developmental stages and diverse hatchling ages whose morphological characteristics have been previously described (Montague et al., 2021).

2.2. Tissue processing

Retinal histogenesis in *S. officinalis* was analysed by scanning electron microscopy (SEM) and light microscopy in semi-thin sections.

2.2.1. SEM study

For SEM study, some *S. officinalis* specimens were fixed in 4% paraformaldehyde (PFA) diluted in 0.1 M phosphate buffer saline (PBS) (pH 7.4) one time for 24 hours at 4 °C and washed three times in the same buffer during 30 minutes each. Then, embryos were immersed overnight in a cryoprotective solution (15% sucrose in PBS) at 4 °C overnight, soaked in embedding medium, and frozen. Specimens were orientated accurately in a cryostat microtome (Leica CM 1900, Charleston, SC, USA) and cryosections of 20 μm were obtained at regular intervals. When the desired plane of sectioning (central region of the eye) was reached, after examination of the sections by a light microscope, the rest of the embryo (still embedded in frozen cryomedia) was transferred to PBS at 4 °C. Then the embryos were processed for SEM. They were additionally fixed in 2.5% glutaraldehyde for 90 min at 4 °C and washed in 0.1 M cacodylate buffer three times during 15 minutes each. Samples were dried by liquid carbon dioxide critical point, gold sputter coated and visualized in a Quanta 3D FEG (ESEM-FIB; FEI Company, Hillsboro, OR, United States).

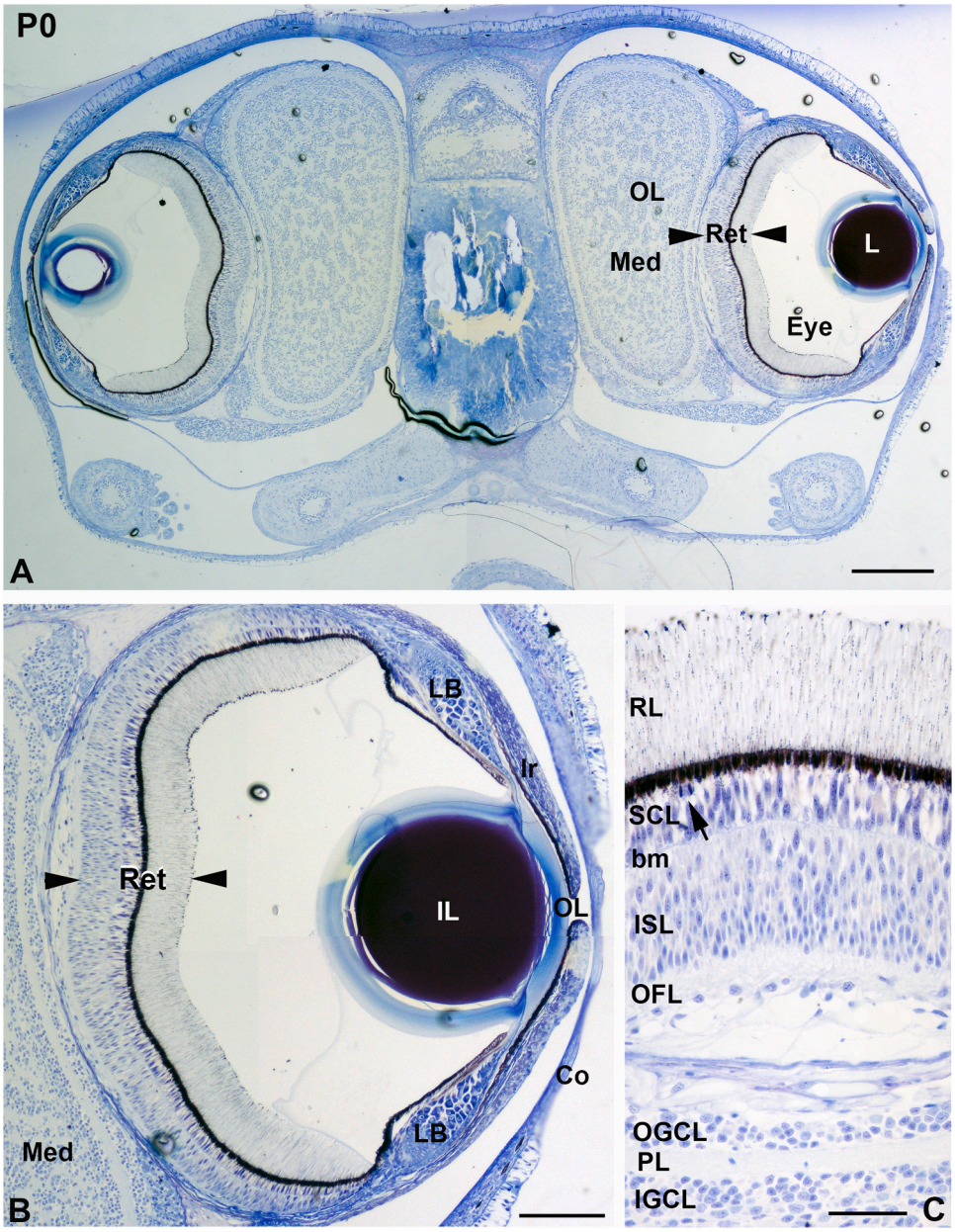

Fig. 3. Toluidine blue-stained semi-thin sections of a newly hatched specimen (P0) of *S. officinalis*, showing the anatomy of the visual system (A), of the eye (B), and retinal and OpL layers (C). Arrowheads point the retinal tissue. (A) The OpL are found close to the eyes, and the L and the Ret are clearly visible. (B) A magnified micrograph of A clearly shows the different parts of the eye: Ret, LB, Ir, and Co. The IL and the OL are clearly distinguished at hatching. (C) The laminar structure of the retina is well established, showing a pigmented RL and a thin darkly pigmented layer at the base of the outer segment of photoreceptors. The nuclei located in the SCL rest on a bm that divides them from the ISL. An OFL is also observed, and adjacent to this fibre layer, the more external layer of the OpL, the OGCL located adjacent to the PL, and finally, the IGCL. *Abbreviations: bm, basal membrane; Co, cornea; IGCL, inner granule cell layer; Ir, iris; IL, inner lens; ISL, Inner segmental layer; LB; lentigenic body; Med; central medulla; OFL, optic fibre layer; OGCL, outer granule cell layer; OL, outer lens; OpL, optic lobe; Ret, retina; PL, plexiform layer; RL, rhabdomeric layer; SCL, supporting cell layer. Scale bars: 250 μm in A; 100 μm in B; 50 μm in C.*

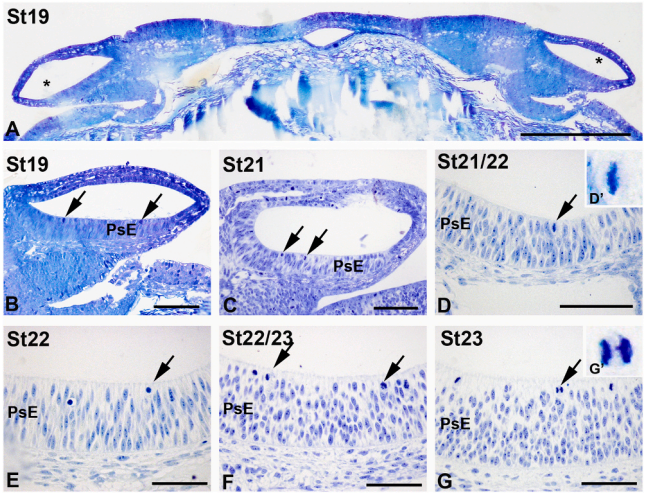

Fig. 4. Toluidine blue-stained semi-thin sections showing early stages of development of the eye rudiment in *S. officinalis*. The eye vesicles are flattened between St19 and St21 (asterisks in A; B,C). The retina is composed of a PsE during these early embryonic stages. Abundant mitotic figures are seen in the apical region of the developing retina (arrows). D' and G' are magnifications of D and G. *Abbreviations: PsE, pseudostratified epithelium. Scale bars: 250 μm in A; 100 μm in B,C; 50 μm in D-G.*

2.2.2. Histological analysis

Some *S. officinalis* embryos and hatchlings were immersed in a mixture of 2% glutaraldehyde and 2% paraformaldehyde in phosphate buffer 0.1 M (PB) for 8 h at 4 ^{o}C. They were rinsed in PB three times during 15 minutes each, postfixed in 2% osmium tetroxide for 2 hours, dehydrated in graded acetone concentrations, rinsed in propylene oxide, and embedded in Spurr's resin. Serial frontal 3 μm semi-thin sections were obtained by a Reichert Jung microtome. The sections were stained with alkaline 1% toluidine blue in 1% aqueous borax, pH 11.0.

2.3. Morphometric analysis

Digital images of retinal sections from developing *S. officinalis* were observed using a Nikon Eclipse-80i photomicroscope equipped with brightfield and fluorescence and photographed using an ultra-high-definition Nikon DXM 1200 F camera. Graphical were performed using Adobe Photoshop (v.CS4). SEM analysis derived images were also utilized for morphometric analysis.

Width measurements of various retinal layers across ocular ontogeny were quantified using ImageJ software (v 1.38) (http://rsb.info.nih.gov/ij/). 20 randomly images per specimen were analysed (three specimens for each developmental phase). Three measurements were taken per section along the apical-basal axis of the central part of the retina, around the eye's main axis.

Statistical analyses were conducted using a Microsoft Excel statistical add-in, XLSTAT, through nonparametric Mann-Whitney U test. Differences between groups were assessed using a null hypothesis (H_0) in which the difference in position between the samples is equal to 0, indicating no difference between them, and an alternative hypothesis (H_a), in which the difference between samples is not equal to 0, representing a significant difference between two samples. Significance level was set at $p < 0.05$.

3. Results

3.1. Anatomy of the S. officinalis visual system: cytoarchitecture of the stratified retina

To understand the retinal structure of the *S. officinalis*, an overview of visual system anatomy and histology is required (Figs. 2 and 3). *S. officinalis* eyes and optic lobes (OpL) are quite voluminous. The eye is mostly spherical and contains all the major structures identified in the vertebrate eyes, namely: cornea (Co), iris (Ir), and pupil. Behind the iris sits a near-spherical lens (L) formed by inner (IL) and outer lens (OL) (Fig. 3A,B) that develop from the lentigenic body (LB).

The OpL are large structures that are easily recognizable just beneath the eye (Fig. 2A,A'; 3 A). They consist of an outer cortex with two layers of cell somata that are called outer granule cell layer (OGCL) and inner granule cell layer (IGCL), separated by a plexiform layer (PL) (Fig. 3B,C). Internally to the cortex, a central medulla (Med) (Fig. 3A,B) comprising clusters of cell bodies surrounded by areas of fibres, neuropil, and fine blood vessels (not shown) is present.

Concerning cephalopod retina, definitions for various layers changed frequently in the literature. The nomenclature used in the present study for the retinal layers has been used in Yamamoto, 1985a, Hao et al. (2010), and Evans et al. (2015). The stratified cephalopod retina is composed of two nuclear layers divided by the basal membrane (bm) (Fig. 2B,B'; 3 C). Photoreceptor cell bodies (Inner Segmental Layer, ISL) are located posterior to the bm (further from the lens), while supporting cell layer (SCL) is found anterior to the bm (closer to the lens) (Fig. 2B,B'; 3 C). In the more internal surface of the SCL (apical surface), mitotic figures can be distinguishable (Fig. 3C). In the more internal layer is located the rhabdomeric layer (RL) containing the outer segments of the photoreceptors (Fig. 2B,B'; 3B,C). A high amount of pigment granules is found at the base of the outer photoreceptor segments (Fig. 3B,C). Externally, the optic fibre layer (OFL) is formed by the photoreceptor cell axons that exit the eye towards the OpL.

3.2. Retinal development in S. officinalis: qualitative study

The eye vesicle is flattened between St19-St21 (Fig. 4A-C), but from St21/22 onwards, gradually become spherical (Figs. 3 and 5–9). Mitotic activity is detected during all the embryonic stages analysed (Figs. 4–8) and even during the first three postnatal weeks of life (Fig. 9). Mitotic figures are always located in the apical surface of the non-laminated retina that is composed of a pseudostratified epithelium (PsE) (Fig. 4), and in the apical surface of the SCL in the laminated retina (Figs. 3, 5–8).

Between St19-St23/24 (E10-E17), the presumptive cuttlefish retina is composed of a PsE (Fig. 4). At St24 the first nuclei passed through narrow breaks of the bm into the incipient ISL (Fig. 5A-D). Therefore, St24 is the onset of the appearance of the photoreceptor cells. At St25 abundant nuclei crossing the bm are distinguishable and an incipient layer of apical processes (the future RL) become visible from the distal margin of the SCL (Fig. 5F). At St25/26 SEM micrographs reveal that the

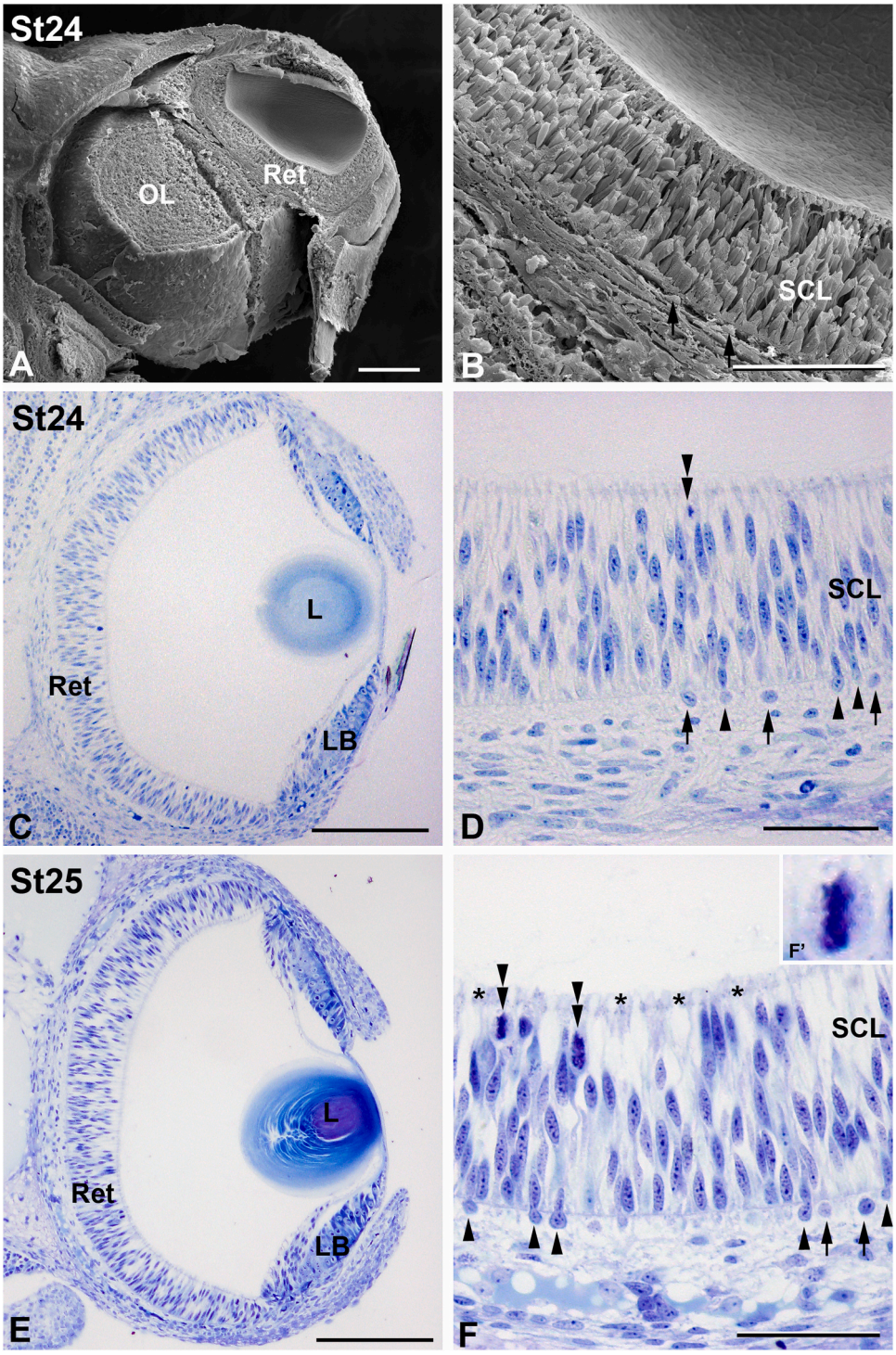

Fig. 5. SEM images (A,B) and toluidine-blue semi-thin sections (C-F) of the *S. officinalis* eye between St24 (A-D) and St25 (E,F). The eye shape is spherical by these stages and the L is clearly visible (A,C,E). Abundant mitotic figures (double arrowheads in D,F) are found in the apical surface of the SCL. The first differentiated photoreceptors are located beneath the bm (arrows in B,D,F), initiating the formation of the ISL. The nuclei of migrating photoreceptor precursors are seen crossing the bm (arrowheads in D,F). Differentiating distal processes of photoreceptors (asterisks in F) are first observed in the apical region of the undifferentiated retina at St25. F' is a magnification of F. *Abbreviations: LB, lentigenic body; OpL, optic lobe; Ret, retina; SCL, supporting cell layer. Scale bars: 250 μm in A; 200 μm in C,E; 50 μm in B, D,F.*

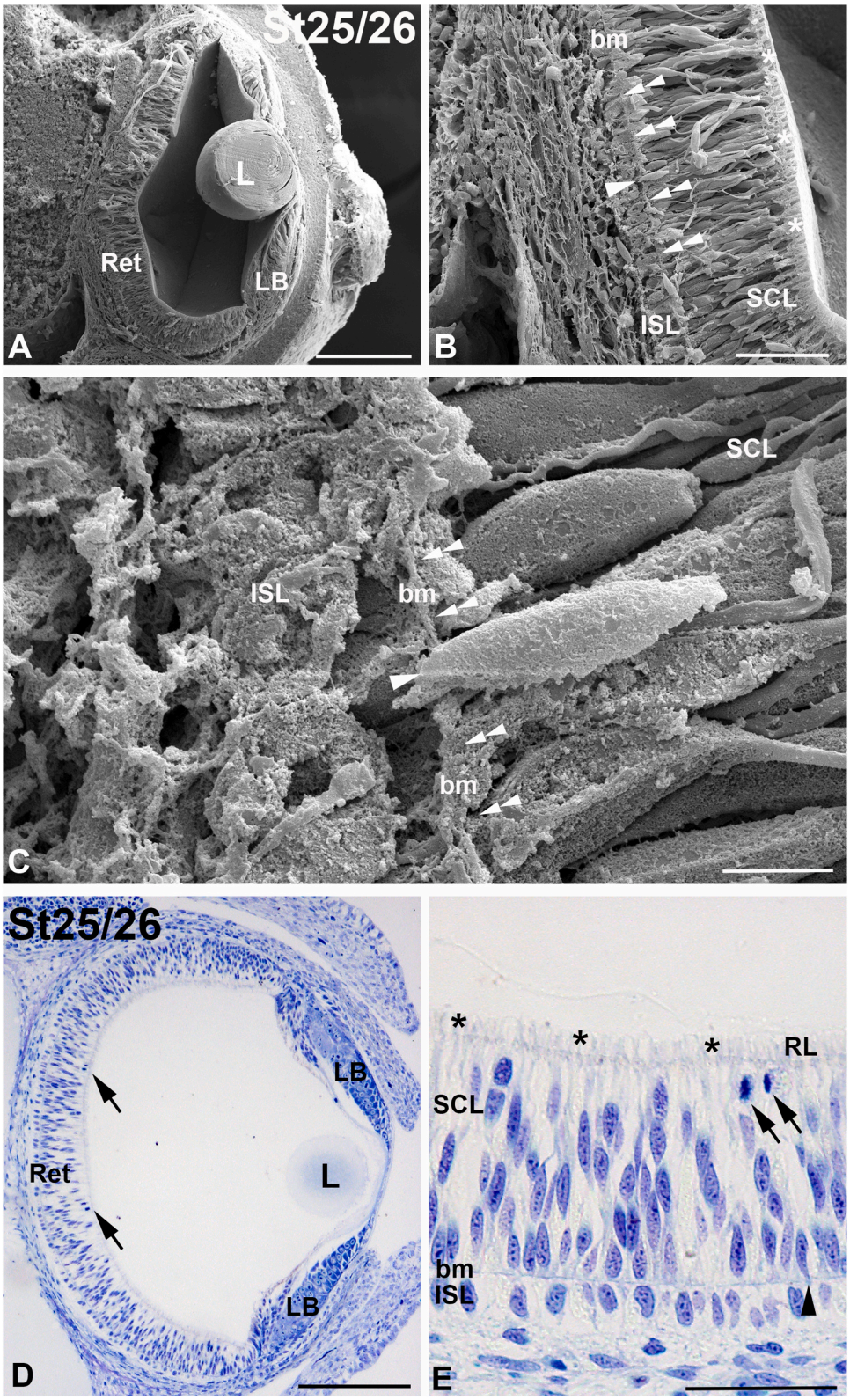

Fig. 6. SEM images (A-C) and toluidine-blue semi-thin sections (D,E) of the developing *S. officinalis* eye at St25/26. The main eye structures (Ret, L, LB) are clearly visible (A,D). The differentiating retina is composed of a SCL and an incipient ISL displaying photoreceptors in a single row (B-E). The nuclei of migrating photoreceptor precursors (arrowheads in B,C,E) are seen crossing the bm (double arrowheads in B,C). Distal processes of photoreceptors (asterisks in B,E) and mitotic figures (arrows in D,E) are found in the apical region of the undifferentiated retina. *Abbreviations: bm, basal membrane; L, lens; LB, lentigenic body; ISL, Inner segmental layer; Ret, retina; RL, rhabdomeric layer; SCL, supporting cell layer. Scale bars: 250 μm in A,D; 50 μm in B,E; 5 μm in C.*

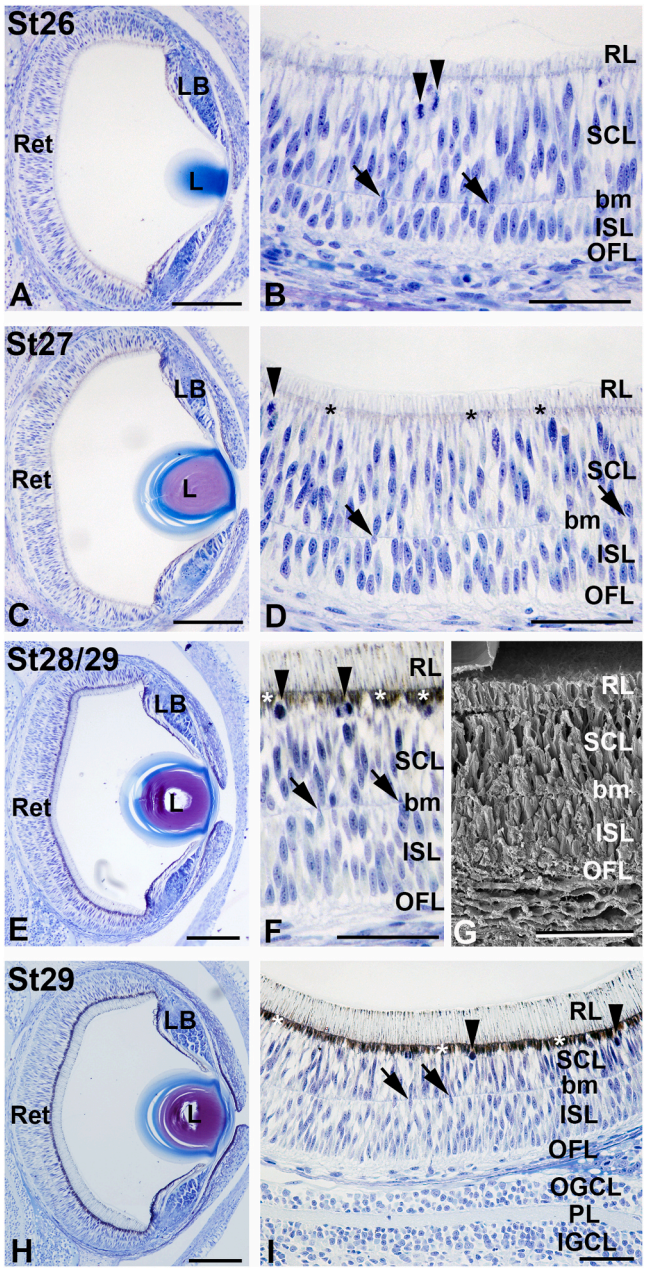

Fig. 7. Toluidine-blue semi-thin sections (A-F,H,I) and a SEM image (G) of the developing *S. officinalis* eye at St26 (A,B), St27 (C,D), St28/29 (E-G), and St29 (H,I). The SCL and the ISL are clearly defined and separated by a bm in all stages shown. The ISL progressively thickens and becomes multilayered as development proceeds (B,D,F,G,I). The onset of pigmentation in the base of the external segment of photoreceptors (asterisks) is detected at St27 (D) and progressively increases and extends to the RL as development proceeds (E,F,H, I). Mitotic activity (arrowheads) is detected in the apical region of the differentiating retina and many photoreceptor precursors are seen crossing the bm (arrows). *Abbreviations: bm, basal membrane; L, lens; LB, lentigenic body; ISL, Inner segmental layer; OFL, optic fibre layer; Ret, retina; RL, rhabdomeric layer; SCL, supporting cell layer. Scale bars: 200 μm in A,C,E,H; 50 μm in B,D,F,G,I.*

ISL and the RL continue to grow, and the presence of some photoreceptor precursors migrating throughout the bm (Fig. 6A-C). These morphological features are corroborated in resin sections (Fig. 6D,E).

Between St26-St29 (Fig. 7) abundant photoreceptor precursors continue to cross the bm (Fig. 7B,D,F,I) and the ISL progressively become multilayered (Fig. 7B,D,F,G,I). At St27, faint pigmentation in the base of RL is firstly observed (Fig. 7D) and become darkly pigmented as development proceeds (Fig. 7E,F,H,I; 8E,F), even after hatching (Fig. 9). Furthermore, pigment granules are distributed in the outer segment of the photoreceptors (RL) from St28/29 onwards (Fig. 7E,F,H, I; 8E,F; 9). During the last embryo stages (Fig. 8) both the RL and the ISL progressively increased in width (Fig. 8B,D-F, see below).

In newly hatched animals, many mitotic figures abut the most apical region of the SCL (Fig. 9B,D,F,H) and migrating photoreceptor precursors pass through the bm are found during the first 3 weeks of life (Fig. 9B,D,F,H). It is important to note that light microscopy observation of toluidine blue-stained semi-thin sections revealed sparse pyknotic bodies mainly in early embryos (see Fig. 4E).

In sum, our data show that proliferative activity is intense throughout the embryonic period and is also observed during the first postnatal weeks. Furthermore, migrating nuclei of photoreceptor precursors crossing the bm are observed even the post hatching stages. The emergence of the ISL and the RL occurs at St24 and at St25 respectively, and the pigmentation of the RL is firstly detected at St27 (see Table 2).

3.3. Retinal development in S. officinalis: quantitative study

Morphometric data on the retinal layers of the embryonic and newly hatched animal retinas are presented in the Fig. 10. Data on the width of the retinal layers are obtained from the central region of each retina. The width of the PsE/SCL increases between St22 and St25/26, but from this stage the thickness of this retinal layer diminishes progressively until the postnatal period, reaching the lowest values between P14 and P21 (Fig. 10A). The thickness of the ISL shows a regular increase between St24 and St29 (Fig. 10B). From this stage onwards, the ISL increases in height irregularly until postnatal stages (Fig. 10B). Finally, the RL increases in height during all embryonic stages analysed, showing a higher increase at the perinatal period and during the first days after hatching, reaching the highest values at P14 (Fig. 10C). Therefore, the width of the RL and the ISL increases during the embryonic period and even during the first postnatal stages, but the thickness of the SCL increases until St25/26 and diminishes progressively until the postnatal period.

4. Discussion

4.1. The retina of S. officinalis hatchlings and juveniles

S. officinalis presents an everted retina with rhabdomeric photoreceptors towards the light, showing a histological organization that closely agrees with that shown in other cephalopod species such as *Octopus vulgaris* (Hanke and Kelber, 2020; Yamamoto et al., 1965), *Octopus minor* (Ryu et al., 2023), *Sepiella japonica* (Yamamoto, 1985b), *Sepia esculenta* (Hao et al., 2010), *Sepiotheutis australis* (Bozzano et al., 2009), *Doryteuthis pealeii* (Koenig et al., 2016).

The typical cytoarchitecture described in the mature retina of cephalopods is clearly visible in hatchlings of *S. officinalis*, but also at late embryonic stages. It has been described that the timing of visual system development has implications for visual system capabilities of newly hatched individuals in fish (Álvarez-Hernán et al., 2019; Bejarano-Escobar et al., 2014; Evans and Browman, 2004) and birds (Álvarez-Hernán et al., 2021). In the case of *S. officinalis,* there is evidence of early visual learning at late embryonic stages (Darmaillacq et al., 2008). These authors have shown that the exposure of cuttlefish embryos to crabs for at least a week before hatching induces a preference for this prey in cuttlefish juveniles. Our results, showing the advanced morphological maturity of the retina of *S. officinalis* at late embryonic stages, support the early acquisition of visual capabilities prior to hatching.

Our data also show features of postnatal neurogenesis in the retina of *S. officinalis,* such as the presence of mitotic figures and the existence of migrating photoreceptors at least in P21 juveniles. Therefore, the retinal progenitors cells located in the in the SCL that give rise to photoreceptors during development remain active after hatching. In the case of

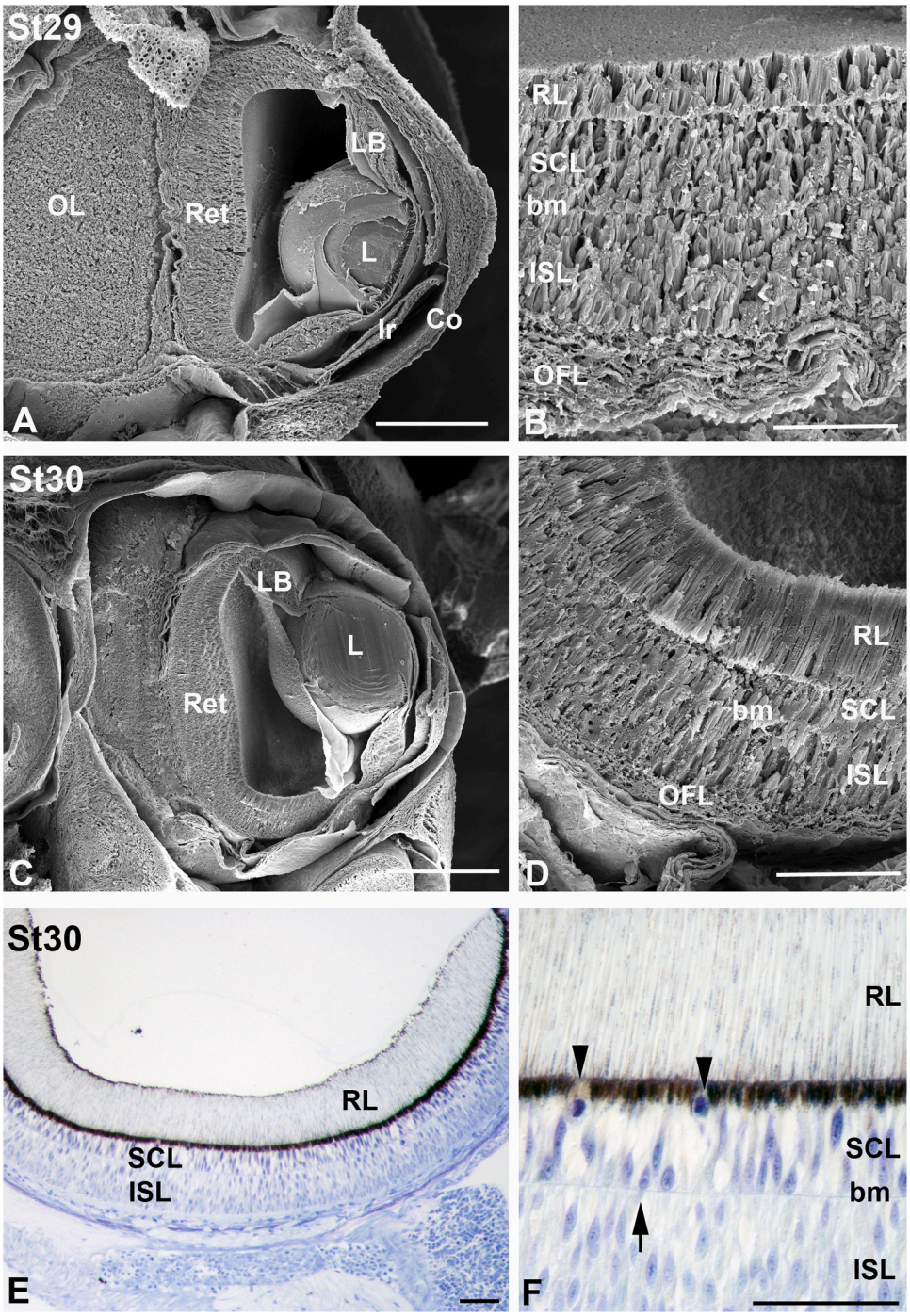

Fig. 8. SEM images (A-D) and toluidine-blue semi-thin sections (E,F) of the developing *S. officinalis* eye during the last embryonic stages: St29 (A,B) and St30 (C-F). The main eye structures are distinguished (A,C) and the retinal layers are clearly established (B,D,E,F). Intense pigmentation is observed in the base of the outer segment of photoreceptors and in the RL (E,F). Mitotic activity (arrowheads) is detected in the apical region of the differentiating retina and photoreceptor precursors are crossing the bm (arrow). *Abbreviations: bm, basal membrane; Co, cornea; L, lens; LB, lentigenic body; Ir, iris; ISL, Inner segmental layer; OFL, optic fibre layer; OpL, optic lobe; Ret, retina; RL, rhabdomeric layer; SCL, supporting cell layer. Scale bars: 250 μm in A,C; 50 μm in B,D-F.*

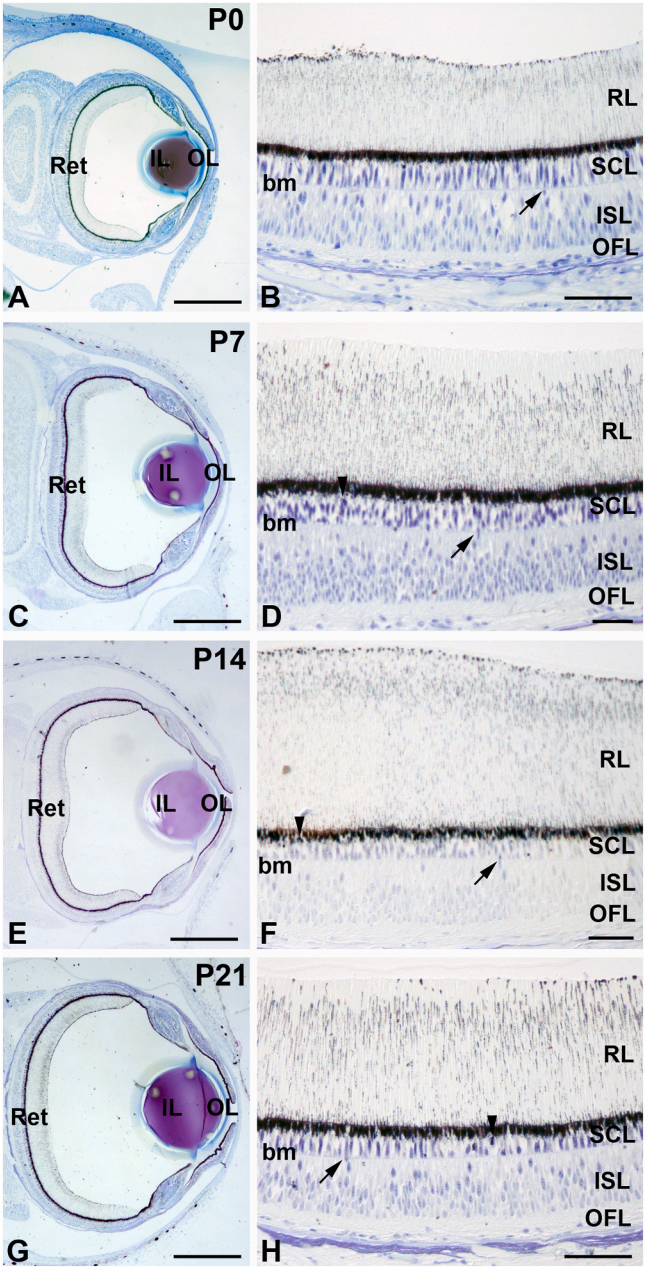

Fig. 9. Toluidine-blue semi-thin sections obtained from retinas of specimens of *S. officinalis* at the time of hatching (A,B), P7 (C,D), P14 (E,F), and P21 (G,H). The main eye structures are distinguished and the OL and the IL are clearly visible (A,C,E,G). The ISL seems to be thicker than the SCL (B,D,F,H). During the first three weeks of life, mitotic activity (arrowheads) and photoreceptor precursors crossing the bm (arrows) are seen in the retina. Intense pigmentation is observed in the base of the outer segment of photoreceptors and in the RL. *Abbreviations: bm, basal membrane; IL, inner lens; ISL, Inner segmental layer; OFL, optic fibre layer; OL, outer lens; Ret, retina; RL, thabdomeric layer; SCL, supporting cell layer. Scale bars: 250 μm in A,C,E,G; 50 μm in B,D,F,H.*

Table 2
Summary of the developmental stages in which takes place the emergence of the different layers and the onset of pigmentation.

Developmental events	Developmental stage
Retina is composed by a PsE	St19-St23/24
Emergence of the ISL	St24
Emergence of the RL	St25
Onset of pigmentation	St27

vertebrates, retinal neurogenesis in mature tissues is detected in the retina of fish (Centanin and Wittbrodt, 2014; Hernández-Núñez et al., 2021; Raymond et al., 2006) and birds (Álvarez-Hernán et al., 2018, 2021, 2022, Fischer and Reh, 2000, 2001; Gallina et al., 2016). In the case of mammals, most retinal adult stem cells are remained in a quiescent state, and therefore postnatal neurogenesis is almost absent (Sokolova et al., 2023).

This neurogenic capacity in the mature retinal tissues in juvenile specimens of cuttlefish could also suggests that under neurodegenerative conditions, these stem cell niches could restore the structure and function of retinal tissue in *S. officinalis*.

4.2. The differentiating retina of S. officinalis: qualitative and quantitative studies

Between St19 (E10) and St23/24 (E17), the *S. officinalis* retina is composed of a columnar epithelium with nuclei positioned at different depths, a highly coincident distribution of nuclei described in the undifferentiated neural tube and retinal neuroepithelia in vertebrates (Bejarano-Escobar et al., 2014; Norden, 2017). Mitotic activity in the developing *S. officinalis* retina occurs on the apical surface, which corresponds to the more internal surface (closer to the lens) of the undifferentiated retina in cephalopods (Imarazene et al., 2017; Koenig et al., 2016; Napoli et al., 2022) and to the more external region (closer to the pigment epithelium) of the retina in vertebrates (Álvarez-Hernán et al., 2018, 2020, 2022). A recent paper has shown that retinal progenitor cells located in the undifferentiated retina of the squid *Doryteuthis pealeii* undergo nuclear migration until they exit the cell cycle (Napoli et al., 2022), similar to the mechanisms of cell proliferation and differentiation described in vertebrates during retinal development (Agathocleous and Harris, 2009; Baye and Link, 2008, 2007) and regeneration (Lahne and Hyde, 2016). Therefore, retinal neurogenesis in the developing retina of cephalopods shows exceptional similarity to vertebrate processes.

The nuclei of differentiating photoreceptors located beneath the bm are firstly detected in *S. officinalis* at St24. From this stage onwards, abundant nuclei passing through the bm by narrow breaks are encountered throughout the entire differentiating retina, as has been described in retinal embryonic tissues in *S. japonica* (hao, 1985), *Sepioteuthis australis* (Bozzano et al., 2009), and *D. pealeii* (Koenig et al., 2016). Yamamoto, 1985a described nuclei passing through the bm even at late stages of development in *S. japonica*, coinciding with our results. At St25 the first signs of photoreceptor morphological differentiation arise and short rhabdomeres become visible in the RL. This early morphological differentiation of photoreceptors, once they are present in the ISL, has also been described in the developing retina of *Sepioteuthis australis* (Bozzano et al., 2009) Romagny et al. (2012) shown that St25 embryos start to respond to light stimuli. These results provide evidences that support our contribution related with the photoreceptor differentiation at the same stage.

Once the retinal layers become visible, morphometric data show an increase in the width of the ISL due to the constant addition of newly differentiated photoreceptors. However, during the embryonic perinatal stages and during the first days of postnatal life, the mean values of the ISL thickness are similar. In contrast, our data show an exponential increase of the thickness of the RL from the embryonic period to the early postnatal life, as has previously been described in *S. japonica* (Yamamoto, 1985a).

In the case of the SCL, the mean values of thickness increased moderately during the early embryonic period, reaching a peak at St25/26. From this stage onwards, the values progressively diminish until early postnatal period. The decrease of the thickness could be related with programmed cell death events during development as described before in several vertebrates (Braunger et al., 2014; Candal et al., 2005; Mayordomo et al., 2003). The continuous thinning of the SCL could be due to the growth of the ocular tissues during the growth phase. Furthermore, during this period, mitotic activity detected in the SCL

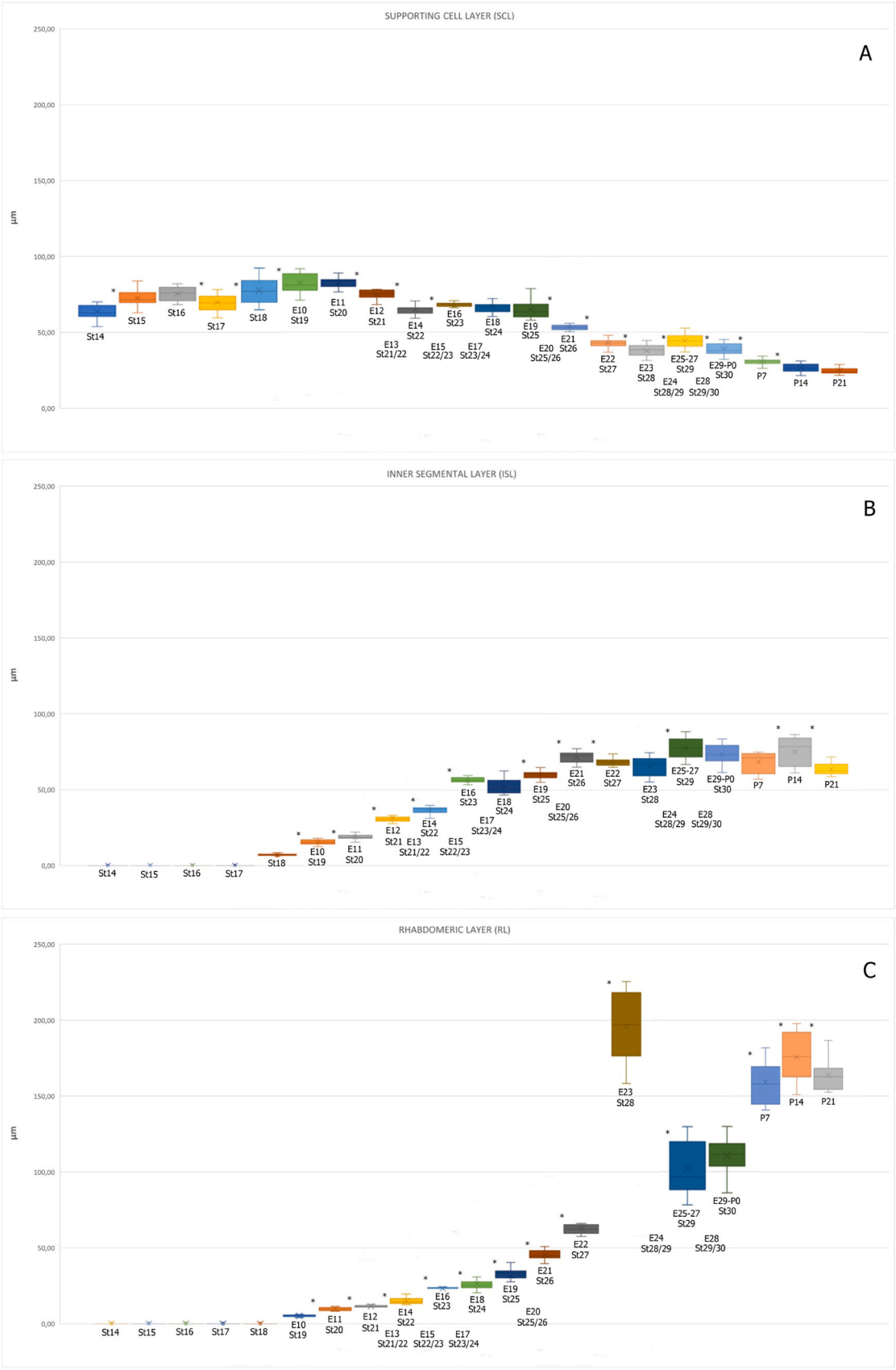

Fig. 10. Quantitative analysis of the variation with time of the thickness of the different *S. officinalis* retinal layers in embryos and postnatal specimens. While the width of the RL and ISL increased with the advance of development and age, the values for the SCL decreases from E20 onwards. Data are expressed as mean ± SEM. Statistical significance is indicated by asterisks (*$p<0.05$).

could be mainly involved in generating precursors of photoreceptors, but not in increasing the number of supporting cells.

5. Conclusions

S. officinalis is an excellent model system to investigate changes in the histological organization of the retina during development. The presence of active neurogenesis after hatching suggests the existence of stem cell niches located in the SCL that could be involved in maintain retinal tissue growth and homeostasis. Although more extensive research is needed to assess the potential of proliferating cells in the postnatal retina of *S. officinalis*. It is known that neurogenesis takes place in octopus adult brain (Di Cosmo et al., 2018) so this work opens a new avenue of investigation regarding regeneration of the nervous system tissue in invertebrates using retinal neurogenesis as a model.

Authors contributions

Alejandro Arias-Montecino, José Antonio de Mera-Rodríguez and Violeta Calle-Guisado carried out experimental procedures, discussed and wrote the manuscript. Antonio Syke provided the embryos and posthacth individuals. Guadalupe Álvarez Hernán, Gervasio Martín-Partido, Joaquín Rodríguez-León and Javier Francisco-Morcillo designed, discussed and wrote the manuscript. This work was supported by grants from the Junta de Extremadura, Fondo Europeo de Desarrollo Regional, "Una manera de hacer Europa" (GR18114, GR21167, IB18113). The authors acknowledge the support of the Servicio.de.Análisis.y.Caracterización.de.Sólidos.y.Superficies.(SACSS) from the Servicios.de.Apoyo.a.la.Investigación.de.la.Universidad.de.Extremadura.(SAIUEX)?.specially to María Carbajo for her excellent technical advice with the SEM.

Ethical statement

All the procedures were approved by *Centro do Ciências do Mar (CCMAR)* and *Direcção-Geral de Alimentação e Veterinária* of the Portuguese Government, according to National (*Decreto-Lei* 113/2013) and EU legislation (Directive 2010/ 63/EU) on the protection of animals used for scientific purposes.

CRediT authorship contribution statement

Javier Francisco-Morcillo: Writing – review & editing, Writing – original draft, Supervision, Methodology, Investigation, Funding acquisition, Data curation, Conceptualization. **Alejandro Arias-Montecino:** Writing – original draft, Methodology, Investigation, Data curation. **Guadalupe Álvarez-Hernán:** Writing – review & editing, Writing – original draft, Supervision, Formal analysis. **Antonio Sykes:** Writing – review & editing, Supervision, Data curation. **Violeta Calle-Guisado:** Writing – review & editing, Methodology, Data curation. **José Antonio De Mera-Rodríguez:** Writing – review & editing, Supervision, Data curation. **Joaquín Rodríguez-León:** Supervision, Writing – review & editing, Data curation, Methodology. **Gervasio Martín-Partido:** Visualization, Software, Data curation, Writing – review & editing.

Data Availability

Data will be made available on request.

Acknowledgements

This work was supported by grants from the Junta de Extremadura, Fondo Europeo de Desarrollo Regional, "Una manera de hacer Europa" (GR18114, GR21167, IB18113). The authors acknowledge the support of the *Servicio de Análisis y Caracterización de Sólidos y Superficies* (SACSS) from the *Servicios de Apoyo a la Investigación de la Universidad de Extremadura* (SAIUEX), specially to María Carbajo for her excellent technical advice with the SEM.

References

Agathocleous, M., Harris, W.A., 2009. From progenitors to differentiated cells in the vertebrate retina. Annu. Rev. Cell Dev. Biol. 25, 45–69. https://doi.org/10.1146/annurev.cellbio.042308.113259.

Álvarez-Hernán, G., Andrade, J.P., Escarabajal-Blázquez, L., Blasco, M., Solana-Fajardo, J., Martín-Partido, G., Francisco-Morcillo, J., 2019. Retinal differentiation in syngnathids: comparison in the developmental rate and acquisition of retinal structures in altricial and precocial fish species. Zoomorphology 138, 371–385. https://doi.org/10.1007/s00435-019-00447-3.

Álvarez-Hernán, G., de Mera-Rodríguez, J., Gañán, Y., Solana-Fajardo, J., Martín-Partido, G., Rodríguez-León, J., Francisco-Morcillo, J., 2021. Development and postnatal neurogenesis in the retina: a comparison between altricial and precocial bird species. Neural Regen. Res. 16, 16. https://doi.org/10.4103/1673-5374.286947.

Álvarez-Hernán, G., de Mera-Rodríguez, J.A., Hernández-Núñez, I., Acedo, A., Marzal, A., Gañán, Y., Martín-Partido, G., Rodríguez-León, J., Francisco-Morcillo, J., 2022. Timing and Distribution of Mitotic Activity in the Retina During Precocial and Altricial Modes of Avian Development. Front. Neurosci. 16, 853544 https://doi.org/10.3389/fnins.2022.853544.

Álvarez-Hernán, G., Hernández-Núñez, I., Rico-Leo, E.M., Marzal, A., de Mera-Rodríguez, J.A., Rodríguez-León, J., Martín-Partido, G., Francisco-Morcillo, J., 2020. Retinal differentiation in an altricial bird species, *Taeniopygia guttata*: an immunohistochemical study. Exp. Eye Res. 190, 107869 https://doi.org/10.1016/j.exer.2019.107869.

Álvarez-Hernán, G., Sánchez-Resino, E., Hernández-Núñez, I., Marzal, A., Rodríguez-León, J., Martín-Partido, G., Francisco-Morcillo, J., 2018. Retinal histogenesis in an altricial avian species, the zebra finch (*Taeniopygia guttata* , Vieillot 1817). J. Anat. 233, 106–120. https://doi.org/10.1111/joa.12809.

Baye, L.M., Link, B.A., 2007. Interkinetic nuclear migration and the selection of neurogenic cell divisions during vertebrate retinogenesis. J. Neurosci. 27, 10143–10152. https://doi.org/10.1523/JNEUROSCI.2754-07.2007.

Baye, L.M., Link, B.A., 2008. Nuclear migration during retinal development. Brain Res. 1192, 29–36. https://doi.org/10.1016/j.brainres.2007.05.021.

Bejarano-Escobar, R., Blasco, M., Martín-Partido, G., Francisco-Morcillo, J., 2014. Molecular characterization of cell types in the developing, mature, and regenerating fish retina. Rev. Fish. Biol. Fish. 24, 127–158. https://doi.org/10.1007/s11160-013-9320-z.

Boletzky, S., Andouche, A., Bonnaud-Ponticelli, L., 2016. A Dev. Table embryogenesis sepia Off. 12. *Vie et Milieu*. 66, 12–23, 02408759.

Bozzano, A., Pankhurst, P.M., Moltschaniwskyj, N.A., Villanueva, R., 2009. Eye development in southern calamary, *Sepioteuthis australis*, embryos and hatchlings. Mar. Biol. 156, 1359–1373. https://doi.org/10.1007/s00227-009-1177-2.

Braunger, B.M., Demmer, C., Tamm, E.R., 2014. Programmed Cell Death During Retinal Development of the Mouse Eye. In: Ash, J.D., Grimm, C., Hollyfield, J.G., Anderson, R.E., LaVail, M.M., Bowes Rickman, C. (Eds.), Retinal Degenerative Diseases, Advances in Experimental Medicine and Biology. Springer New York, New York, NY, pp. 9–13. https://doi.org/10.1007/978-1-4614-3209-8_2.

Buresi, A., Baratte, S., Da Silva, C., Bonnaud, L., 2012. orthodenticle/otx ortholog expression in the anterior brain and eyes of *Sepia officinalis* (Mollusca, Cephalopoda). Gene Expr. Patterns 12, 109–116. https://doi.org/10.1016/j.gep.2012.02.001.

Buresi, A., Canali, E., Bonnaud, L., Baratte, S., 2013. Delayed and asynchronous ganglionic maturation during cephalopod neurogenesis as evidenced by *Sof*-elav1 expression in embryos of *Sepia* officinalis (Mollusca, Cephalopoda). J. Comp. Neurol. 521, 1482–1496. https://doi.org/10.1002/cne.23231.

Candal, E., Anadón, R., DeGrip, W.J., Rodríguez-Moldes, I., 2005. Patterns of cell proliferation and cell death in the developing retina and optic tectum of the brown trout. Dev. Brain Res. 154, 101–119. https://doi.org/10.1016/j.devbrainres.2004.10.008.

Centanin, L., Wittbrodt, J., 2014. Retinal neurogenesis. Development 141, 241–244. https://doi.org/10.1242/dev.083642.

Darmaillacq, A.-S., Lesimple, C., Dickel, L., 2008. Embryonic visual learning in the cuttlefish, Sepia officinalis. Anim. Behav. 76, 131–134. https://doi.org/10.1016/j.anbehav.2008.02.006.

Di Cosmo, A., Bertapelle, C., Porcellini, A., Polese, G., 2018. Magnitude assessment of adult neurogenesis in the octopus vulgaris brain using a flow cytometry-based technique. Front. Physiol. 9, 1050. https://doi.org/10.3389/fphys.2018.01050.

Evans, A.B., Acosta, M.L., Bolstad, K.S., 2015. Retinal development and ommin pigment in the Cranchiid Squid Teuthowenia pellucida (Cephalopoda: Oegopsida). PLOS ONE 10, e0123453. https://doi.org/10.1371/journal.pone.0123453.

Evans, B., Browman, H., 2004. Variation in the development offish retina. American Fishe. Soc. Symp. 40, 145–166, p. 21.

Fischer, A.J., Reh, T.A., 2000. Identification of a proliferating marginal zone of retinal progenitors in postnatal chickens. Dev. Biol. 220, 197–210. https://doi.org/10.1006/dbio.2000.9640.

Fischer, A.J., Reh, T.A., 2001. Müller glia are a potential source of neural regeneration in the postnatal chicken retina. Nat. Neurosci. 4, 247–252. https://doi.org/10.1038/85090.

Francisco-Morcillo, J., Bejarano-Escobar, R., Rodríguez-León, J., Navascués, J., Martín-Partido, G., 2014. Ontogenetic cell death and phagocytosis in the visual system of vertebrates. Dev. Dyn. 243, 1203–1225. https://doi.org/10.1002/dvdy.24174.

Gallina, D., Palazzo, I., Steffenson, L., Todd, L., Fischer, A.J., 2016. β-catenin-signaling and the formation of Müller glia-derived progenitors in the chick retina. Dev. Neurobiol. 76, 983–1002. https://doi.org/10.1002/dneu.22370.

Hanke, F.D., Kelber, A., 2020. The eye of the common octopus (*Octopus vulgaris*). Front. Physiol. 10, 1637. https://doi.org/10.3389/fphys.2019.01637.

Hao, Z.-L., Zhang, X.-M., Kudo, H., Kaeriyama, M., 2010. Development of the Retina in the Cuttlefish *Sepia* esculenta. J. Shellfish Res. 29, 463–470. https://doi.org/10.2983/035.029.0224.

Harris, W.A., 1997. *Pax*-6: Where to be conserved is not conservative. Proc. Natl. Acad. Sci. 94, 2098–2100. https://doi.org/10.1073/pnas.94.6.2098.

Hernández-Núñez, I., Quelle-Regaldie, A., Sánchez, L., Adrio, F., Candal, E., Barreiro-Iglesias, A., 2021. Decline in constitutive proliferative activity in the zebrafish retina with ageing. Int. J. Mol. Sci. 22, 11715. https://doi.org/10.3390/ijms222111715.

Imarazene, B., Andouche, A., Bassaglia, Y., Lopez, P.-J., Bonnaud-Ponticelli, L., 2017. Eye development in sepia officinalis embryo: what the uncommon gene expression profiles tell us about eye evolution. Front. Physiol. 8, 613. https://doi.org/10.3389/fphys.2017.00613.

Koenig, K.M., Gross, J.M., 2020. Evolution and development of complex eyes: a celebration of diversity. Development 147, dev182923. https://doi.org/10.1242/dev.182923.

Koenig, K.M., Sun, P., Meyer, E., Gross, J.M., 2016. Eye development and photoreceptor differentiation in the cephalopod *Doryteuthis* pealeii. Development, dev.134254. https://doi.org/10.1242/dev.134254.

Kolb, H., Nelson, R., Ahnelt, P., Cuenca, N., 2001. Chapter 1 Cellular organization of the vertebrate retina. in: Progress in Brain Research. Elsevier, pp. 3–26. https://doi.org/10.1016/S0079-6123(01)31005-1.

Lahne, M., Hyde, D.R., 2016. Interkinetic Nuclear Migration in the Regenerating Retina. In: Bowes Rickman, C., LaVail, M.M., Anderson, R.E., Grimm, C., Hollyfield, J., Ash, J. (Eds.), Retinal Degenerative Diseases. Springer International Publishing, Cham, pp. 587–593. https://doi.org/10.1007/978-3-319-17121-0_78.

Lemaire, J., 1970. Table de développement embryonnaire de. Sepia Off. 95, 9. *Bullet Soc Zoo France*. 95, 773-782. ISSN:0037-962X.

Mangold-Wirz, K., 1963. Biologie des Céphalopodes benthiques et nectoniques de la Mer Catalane.

Mayordomo, R., Valenciano, A.I., De La Rosa, E.J., Hallböök, F., 2003. Generation of retinal ganglion cells is modulated by caspase-dependent programmed cell death. Eur. J. Neurosci. 18, 1744–1750. https://doi.org/10.1046/j.1460-9568.2003.02891.x.

Montague, T.G., Rieth, I.J., Axel, R., 2021. Embryonic development of the camouflaging dwarf cuttlefish, *Sepia bandensis*. Dev. Dyn. 250, 1688–1703. https://doi.org/10.1002/dvdy.375.

Moreno-Marmol, T., Cavodeassi, F., Bovolenta, P., 2018. Setting eyes on the retinal pigment epithelium. Front. Cell Dev. Biol. 6, 145. https://doi.org/10.3389/fcell.2018.00145.

Napoli, F.R., Daly, C.M., Neal, S., McCulloch, K.J., Zaloga, A.R., Liu, A., Koenig, K.M., 2022. Cephalopod retinal development shows vertebrate-like mechanisms of neurogenesis. Curr. Biol. 32, 5045–5056.e3. https://doi.org/10.1016/j.cub.2022.10.027.

Nilsson, D.-E., Johnsen, S., Warrant, E., 2023. Cephalopod versus vertebrate eyes. Curr. Biol.: CB 33, R1100–R1105. https://doi.org/10.1016/j.cub.2023.07.049.

Norden, C., 2017. Pseudostratified epithelia – cell biology, diversity and roles in organ formation at a glance. J. Cell Sci. jcs 192997. https://doi.org/10.1242/jcs.192997.

Petridou, E., Godinho, L., 2022. Cellular and molecular determinants of retinal cell fate. Annu. Rev. Vis. Sci. 8, 79–99. https://doi.org/10.1146/annurev-vision-100820-103154.

Raymond, P.A., Barthel, L.K., Bernardos, R.L., Perkowski, J.J., 2006. Molecular characterization of retinal stem cells and their niches in adult zebrafish. BMC Dev. Biol. 6, 36. https://doi.org/10.1186/1471-213X-6-36.

Romagny, S., Darmaillacq, A.-S., Guibé, M., Bellanger, C., Dickel, L., 2012. Feel, smell and see in an egg: emergence of perception and learning in an immature invertebrate, the cuttlefish embryo. J. Exp. Biol. 215, 4125–4130. https://doi.org/10.1242/jeb.078295.

Ryu, K.-B., Jo, G.-H., Gil, Y.-C., Jeon, D., Choi, N.-R., Jung, S.-H., Jo, S., An, H.S., Lee, H.-Y., Eyun, S., Cho, S.-J., 2023. Eye development and developmental expression of crystallin genes in the long arm octopus, Octopus minor. Front. Mar. Sci. 10, 1136602 https://doi.org/10.3389/fmars.2023.1136602.

Sokolova, N., Zilova, L., Wittbrodt, J., 2023. Unravelling the link between embryogenesis and adult stem cell potential in the ciliary marginal zone: a comparative study between mammals and teleost fish. Cells Dev. 174, 203848 https://doi.org/10.1016/j.cdev.2023.203848.

Sykes, A.V., Baptista, F.D., Gonçalves, R.A., Andrade, J.P., 2012. Directive 2010/63/EU on animal welfare: a review on the existing scientific knowledge and implications in cephalopod aquaculture research. Rev. Aquac. 4, 142–162. https://doi.org/10.1111/j.1753-5131.2012.01070.x.

Sykes, A.V., Domingues, P.M., Andrade, J.P., 2006. Effects of Using Live Grass Shrimp (Palaemonetes varians) as the only Source of Food for the Culture of Cuttlefish, Sepia officinalis (Linnaeus, 1758). Aquac. Int. 14, 551–568. https://doi.org/10.1007/s10499-006-9054-1.

Tomarev, S.I., Callaerts, P., Kos, L., Zinovieva, R., Halder, G., Gehring, W., Piatigorsky, J., 1997. Squid Pax-6 and eye development. Proc. Natl. Acad. Sci. 94, 2421–2426. https://doi.org/10.1073/pnas.94.6.2421.

Wentworth, S.L., Muntz, W.R.A., 1992. Development of the eye and optic lobe of *Octopus*. J. Zool. 227, 673–684. https://doi.org/10.1111/j.1469-7998.1992.tb04423.x.

Yamamoto, M., 1985a. Ontogeny of the visual system in the cuttlefish, Sepiella japonica. I. Morphological differentiation of the visual cell. J. Comp. Neurol. 232, 347–361. https://doi.org/10.1002/cne.902320307.

Yamamoto, M., 1985b. Ontogeny of the visual system in the cuttlefish, Sepiella japonica. I. Morphological differentiation of the visual cell. J. Comp. Neurol. 232, 347–361. https://doi.org/10.1002/cne.902320307.

Yamamoto, T., Tasaki, K., Sugawara, Y., Tonosaki, A., 1965. Fine structure of the octopus retina. J. Cell Biol. 25, 345–359. https://doi.org/10.1083/jcb.25.2.345.